Liquid-Liquid and Liquid-Gas Extraction of Aroma Compounds with Hollow Fibers

Fabrice Gascons Viladomat, Isabelle Souchon, François-Xavier Pierre, and Michèle Marin
UMR Génie et Microbiologie des Procédés Alimentaires, Institut National de la Recherche Agronomique INRA- INA PG, 78 850 Thiverval Grignon, France

DOI 10.1002/aic.10827
Published online March 27, 2006 in Wiley InterScience (www.interscience.wiley.com).

The extraction of 15 aroma compounds from a highly diluted aqueous feed with hollow fiber membrane contactors was investigated. Membrane-Based Solvent Extraction (MBSE) and Membrane Air-Stripping (MAS) were tested with the aqueous feed cross-flowing on the shell side and the stripping phase flowing in the lumen of the hollow fiber. Experimental results showed that globally, MBSE offered higher overall mass transfer coefficients than MAS. This difference was mainly explained by the gap in partition coefficients. Hexane-water partition coefficients were about 10,000 times higher than air-water partition coefficients. The contribution of each local resistance to mass transfer was identified by a resistance-in-series model. Mass transfer in the aqueous feed boundary layer is the limiting step in MBSE, while mass transfer in the stripping gas boundary layer is the limiting step in MAS. A diagnostic tool based on partition coefficients was developed in order to help choose the adequate process for the extraction of an aroma compound.
 AIChE J, 52: 2079–2088, 2006
Keywords: membrane-based solvent extraction, membrane air-stripping, membrane contactor, mass transfer, physicochemical properties

Introduction

Aroma extracts are widely used in the food industry to improve the flavor of formulated foods or to compensate for the flavor losses of natural raw products during industrial processing. Food industries and aroma manufacturers are thus seeking technologies that allow the selective recovery of aroma compounds from odorous wastewater. Aroma compounds are small molecules (MW $< 300 g \cdot mol^{-1}$) that cover a wide range of chemical classes. Due to their various levels of volatility and hydrophobicity, distillation and liquid-liquid extraction, respectively, cover the majority of industrial applications.[1]

However, traditional techniques suffer from several limitations, which has motivated the search for highly efficient and low-cost alternative technologies. These technologies must be able to operate at moderate temperatures because of the heat sensitivity of some of the aroma compounds and the need for low energy consumption. Moreover, these installations have to be compact in order to be easily integrated into existing industrial facilities. Compactness and low energy consumption are characteristic of membrane processes. Consequently, they have been investigated in this article as a potentially promising technique.

More than 20 years of studies have shown the high potential of membrane contactors for extracting organic molecules from aqueous feeds. According to Gabelman and Hwang,[2] a membrane contactor is a device that achieves liquid/liquid or gas/liquid mass transfer without dispersion of one phase within another. As a consequence, the extracting phase should either be an organic solvent[3-6] (or edible oil[7,8]), air,[9-12] or even a dense gas.[13-15]

The objective of this article is to compare Membrane-Based Solvent Extraction (MBSE) and Membrane Air-Stripping (MAS) for the extraction of aroma compounds from an aqueous solution. Both these techniques were performed using the same type of hydrophobic Hollow Fiber Contactor (HFC) as a

Correspondence concerning this article should be addressed to I. Souchon at souchon@grignon.inra.fr.

vehicle for mass transfer. Hollow fiber geometry was chosen since it offers the largest exchange area per volume unit (surface to volume ratio, a $\approx$ 3000 $m^2 \cdot m^{-3}$). Furthermore, the aqueous feed phase was chosen to flow on the shell side of the HFC since this configuration offers a larger exchange area than the lumen-fed configuration.

MBSE and MAS have been considered for the extraction of 15 aroma compounds with diverse physicochemical properties from a highly diluted aqueous stream. Mass transfer was modeled using a resistance-in-series approach. This model made it possible to draw conclusions about the differences and similarities between the two techniques and, consequently, to build a diagnosis based on the physicochemical properties of the molecules as a tool in helping to choose an adapted membrane-based separation process (MBSE or MAS).

Theory

General equations and main parameters

Unit operations of extraction are governed by a difference in chemical potentials (generally expressed as a difference of concentrations) between the bulk of a solution and the interface. As a result, the mass transfer rate of a compound ($\dot{m}$, $kg \cdot s^{-1}$) can be defined by Eq. 1:

$$\dot{m} = K_f \cdot A_f \cdot (C_f - C_f^*) \tag{1}$$

where K_f is the overall mass transfer coefficient ($m \cdot s^{-1}$) of the compound based on the aqueous feed phase concentration, A_f the outer surface area of the fibers (m^2) since the aqueous feed phase cross flows on the shell side, C_f the concentration of the compound in the aqueous phase ($kg \cdot m^{-3}$), and C_f^* the concentration at the feed/stripping phase interface ($kg \cdot m^{-3}$). C_f^* is an equilibrium concentration in the liquid phase and can be as expressed through the partition coefficient (P), defined as:

$$P = \left[\frac{C_s}{C_f}\right]_{\text{at equilibrium}} \tag{2}$$

where C_s is the concentration ($kg \cdot m^{-3}$) of the compound in the stripping phase (gas or solvent).

Since hexane was chosen as the solvent for the extraction in MBSE, the partition coefficient will be referred to as $P_{hexane/water}$. In the case of MAS, the air-water partition in the infinite dilution range is commonly known as the Henry's law constant (H).

Determining K_f leads to a quantification of the efficiency of the extraction process for each molecule, independently of the driving force. Experimental overall mass transfer coefficients were determined using methods described by D'Elia et al.[16] and Mahmud et al.[17] for MBSE and MAS, respectively. Their approaches are based on local mass balances for a solute between the feed phase and the stripping phase, integrated for a parallel flow counter-current configuration. Estimated mass transfer coefficients are apparent mass transfer coefficients, since the flow on the shell side is a mix of cross and counter-current flow because of the presence of a baffle.

Mass transfer coefficient modeling

Mass transfer in MAS involves three sequential steps. First, molecules diffuse from the bulk of the aqueous feed phase through the aqueous feed boundary layer, and then into the stripping phase-filled pores (since the membrane is hydrophobic) and, finally, diffuse through the stripping phase film. The overall mass transfer resistance ($1/K_f$) results from the cumulative effect of the three local mass transfer resistances, with:

$$\frac{1}{K_f \cdot A_f} = \frac{1}{A_f \cdot k_f} + \frac{1}{\overline{A_m} \cdot k_m \cdot P} + \frac{1}{A_s \cdot k_s \cdot P} \tag{3}$$

where k_f, k_m, and k_s are the local mass transfer coefficients ($m \cdot s^{-1}$) in the aqueous feed phase, in the membrane, and in the stripping phase, respectively; A_s is the inner membrane surface area (m^2) since the stripping phase flows in the fibers; and $\overline{A_m}$ is the mean surface area of the membrane (m^2).

The local mass transfer coefficients can be represented with the dimensionless Sherwood number, which compares the intensity of convective and diffusive mass transfer, according to Eq. 4:

$$k_i = \frac{D \cdot Sh}{d} \tag{4}$$

where k_i is the local mass transfer coefficient ($m \cdot s^{-1}$), D the diffusion coefficient of the solute in the considered phase ($m^2 \cdot s^{-1}$), Sh the dimensionless Sherwood number, and d the diameter (m) of the considered compartment.

The Sherwood number is usually given by an empirical relationship with two other dimensionless numbers: the Reynolds number (Re), which characterizes the flow of the fluid, and the Schmidt number (Sc), which is independent of the flow but characteristic of the solute/solvent couple, according to the following equation:

$$Sh = x \cdot \mathrm{Re}^y \cdot Sc^z \tag{5}$$

with $\mathrm{Re} = (u \cdot d/\nu)$ and $Sc = (\nu/D)$, where u is the velocity of the fluid ($m \cdot s^{-1}$), ν its kinematic viscosity ($m^2 \cdot s^{-1}$), and x, y, z constants characteristic of the experimental range of validation.

Correlations have been validated for the study of heat transfer in cross-flow heat exchangers (with the same geometry as HFCs) and have been successfully used by several authors for mass transfer in hollow fiber membrane contactors as detailed below. The forms of the relationships depend on the layer considered: on the shell side, inside the fibers, or in the pores of the membrane.

Local mass transfer on the shell side

When the aqueous feed flows on the shell side, the Kreith and Black relation,[18] developed for low void fraction heat exchangers and for $\mathrm{Re} < 2000$, was successfully used in membrane-based solvent extraction[5,19] and membrane air-stripping[11,17,20,21] mass transfer modeling.

$$Sh = 0.39 \cdot \mathrm{Re}^{0.59} \cdot Sc^{0.33} \tag{6}$$

leading to a determination of k_f by the following equation:

$$k_f = 0.39 \cdot \mathrm{Re}^{0.59} \cdot Sc^{0.33} \cdot \left(\frac{D_f}{d_h}\right) \tag{7}$$

where D_f is the diffusion coefficient of the aroma compound in the aqueous feed phase ($m^2 \cdot s^{-1}$) and d_h the hydraulic diameter of the hollow fiber (m).

Local mass transfer in the fibers

The general relation proposed by Graetz,[22] which is valid for a fluid flowing in tubes, can be used:

$$Sh = 0.5 \cdot Gz \cdot \left(\frac{1-\zeta}{1+\zeta}\right) \tag{8}$$

with

$$\zeta = \sum_{n=1}^{\infty} -4 \cdot \left(\frac{B_n}{\beta_n^2}\right) \cdot \left(\frac{d\phi}{dr_+}\right)_{r_+=1} \cdot \exp\left(\frac{-2 \cdot \beta_n^2}{Gz}\right)$$

$$\beta_n = 4 \cdot (n-1) + 2.666;\ n = 1, 2, 3, \ldots$$

$$-B_n \left(\frac{d\phi}{dr_+}\right)_{r_+=1} = 2 \cdot (1.01276 \cdot \beta_n^{-0.33})$$

where Gz is the dimensionless Graetz number ($Gz = \mathrm{Re} \cdot Sc \cdot (d/L)$).

Since this expression is not easy to work with, other simpler relationships were investigated. For example, Lévêque[23] developed a specific solution for the Graetz solution in the restricted range of the laminar flows:

$$Sh = 1.62 \cdot Gz^{0.33} \tag{9}$$

However, mass transfer is overestimated for low Graetz numbers using Eq. 9.[11] The limit of validity of the Lévêque solution differs in the literature. Some authors propose Gz = 4,[2] while others propose Gz = 25[24] or even Gz = 400.[25]

For low Gz numbers, another relation can be found by looking at the limits of the Graetz solution (Eq. 8) when Gz→0:

$$\lim_{Gz \to 0}(Sh) = 0.5 \cdot Gz \tag{10}$$

since

$$\lim_{Gz \to 0}(\zeta) = \lim_{Gz \to 0}\left[\sum_{n=1}^{\infty} -4 \cdot \left(\frac{B_n}{\beta_n^2}\right) \cdot \left(\frac{d\phi}{dr_+}\right)_{r_+=1} \cdot \exp\left(\frac{-2 \cdot \beta_n^2}{Gz}\right)\right] = 0$$

Souchon et al.[26] showed that Eqs. 9 and 10 intersect at Gz = 6. Furthermore, Eqs. 9 and 10 are very close to Eq. 8 for Gz < 6 and Gz > 6, respectively.

Consequently, we used the Lévêque solution (Eq. 9) in this study when Gz > 6, and the limit of the general Graetz solution (Eq. 10) when Gz < 6. This makes it possible to determine the local mass transfer coefficient in the fibers, with:

$$k_s = 0.5 \cdot \mathrm{Re} \cdot Sc \cdot \frac{D_s}{L} \quad \text{for} \quad Gz < 6 \tag{11}$$

$$k_s = 1.62 \cdot \left(\mathrm{Re} \cdot Sc \cdot \frac{D_s^3}{L \cdot d^2}\right)^{0.33} \quad \text{for} \quad Gz > 6 \tag{12}$$

where D_s is the diffusion coefficient of the aroma compound in the stripping phase ($m^2 \cdot s^{-1}$).

Local mass transfer in the membrane

The diffusion mechanism of the aroma compounds in the pores of the membrane can be considered as molecular diffusion since Knudsen diffusion is negligible.

Consequently, the local mass transfer is estimated considering that the stripping phase is immobile in the pores of the membrane. According to the work of Kiani et al.[3] on MBSE, the membrane mass transfer coefficient is predicted as:

$$k_m = \frac{D_s \cdot \varepsilon}{\tau \cdot e} \tag{13}$$

where ε and τ are the membrane porosity (dimensionless) and tortuosity (dimensionless), respectively, and e the membrane thickness (m).

Materials and Methods

Aroma compounds

The 15 aroma compounds studied, which are highly representative of specific odors in the flavor and fragrances industries, belong to diverse chemical classes (three esters, three terpene alcohols, two sulfur compounds, two alcohols, two aldehydes, one ketone, one lactone, and one pyrazine). The diversity of the chemical structures offers a large spectrum of physico-chemical properties. Their main characteristics and properties available in the literature are reported in Table 1.

n-Hexane was chosen as the MBSE extracting solvent for several practical reasons. First, it is almost insoluble in water and aroma compounds are highly soluble in n-hexane. Second, it is authorized in food processing and is widely used in aroma compound manufacturing. Given that its boiling point (BP = 69°C) is much lower than the boiling points of the aroma compounds studied, the recovery of these solutes may be based on a simple distillation. n-Hexane can, therefore, be considered as a reference solvent. Capillary grade (98%+) n-hexane was supplied by Carlo Erba, and used as such.

The model solution was obtained by preparing 1L of a concentrated solution in RO water (100 $mg \cdot L^{-1}$ and 600 $mg \cdot L^{-1}$ of each aroma compound for MBSE and MAS, respectively), which was then introduced into the pilot plant reservoir. Water was then added to the feed reservoir in order to obtain 5L (for MBSE experiments) or 30L (for MAS experiments) of the model solution containing the 15 aroma compounds at $\sim 2.10^{-2}$ $kg \cdot m^{-3}$ each. All compounds are soluble in water for

Table 1. Main Characteristics and Properties of the 15 Aroma Compounds Studied in MAS and MBSE

Molecule	CAS	Supplier	Purity (%)	MW[a] (g · mol^{-1})	BP[b] (°C)	Log P[c]	Odor
2.5-Dimethylpyrazine	123-32-0	Acros Organics	99	108.1	155	1.03	Chocolate, earthy
2-Heptanone	110-43-0	Acros Organics	98	114.2	150	1.73	Soapy, fruity
Benzaldehyde	100-52-7	Aldrich	99+	106.1	179	1.71	Almond-like
cis-3-Hexenol	928-96-1	Aldrich	98	100.2	156	1.61	Leaf-like
Dimethyldisulfide	624-92-0	Aldrich	99	94.2	110	1.87	Cabbage-like
Dimethyltrisulfide	3658-80-8	Acros Organics	98+	126.2	177	1.87	Sulfury, pungent
Ethyl butyrate	105-54-4	Aldrich	99	116.2	126	1.85	Fruity
Ethyl hexanoate	123-66-0	Aldrich	99+	144.2	168	2.83	Fruity, pineapple
γ-Decalactone	706-14-9	IFF	–	170.3	281	2.57	Fatty, peach-like
Hexanal	66-25-1	Aldrich	98	100.2	131	1.80	Tallowy, leaf-like
Hexanol	111-27-3	Lancaster	99	102.2	156	1.82	Green, grass
Isoamyl acetate	123-92-2	Aldrich	99+	130.2	142	2.26	Fruity, banana
Isoamyl alcohol	123-51-3	Sigma	99.4	88.1	130	1.26	Malty
Linalool	78-70-6	Aldrich	97	154.2	199	3.38	Flowery
Terpineol	98-55-5	Sigma	95	154.3	218	3.33	Lilac, pine

[a] Molecular weight.
[b] Boiling point at normal pressure.
[c] Log of the octanol/water partition coefficient at 25°C estimated using a group contribution method.[27]

the temperatures and concentrations used in this study. The feed solution was then analyzed by gas chromatography in order to assess the exact concentration of each solute. Due to their low concentration, aroma compounds can be considered in the infinite dilution range, which means no interaction between solutes occurs.

Partition coefficients

Partition coefficients of the 15 aroma compounds between n-hexane and water ($P_{hexane/water}$, -) and between air and water (H, -) were determined at 25°C.

The method developed by Pierre et al.[8] was used for the determination of $P_{hexane/water}$. This method is based on the determination of the solute concentrations in each phase, water and hexane, when equilibrium is reached.

The Phase Ratio Variation (PRV) method[28] was used for the determination of H. This method is based on the analysis of the head-space concentrations of the solutes in equilibrium with an aqueous solution.[21]

Diffusion coefficients

Diffusion coefficients of the 15 aroma compounds were estimated using the Wilke and Chang method[29] in water, n-hexane, and air, at 25°C (Table 2). Diffusion coefficients depend mainly on the viscosity of the phase, explaining the higher values obtained in air ($\mu = 2.10^{-5}$ kg·m^{-1}·s^{-1} at 25°C), rather than in n-hexane ($\mu = 3.10^{-4}$ kg·m^{-1}·s^{-1} at 25°C) or in water ($\mu = 9.10^{-4}$ kg·m^{-1}·s^{-1} at 25°C).

Analytical methods

After the addition of an internal standard (1-Octanol), samples were analyzed by gas chromatography (Hewlett-Packard 6890 series) using an automatic sampler CombiPal (CTC Analytics, Switzerland) and a flame ionization detector (FID). The temperature of the column (Innowax, Hewlett-Packard, d_i = 0.53 mm, d_f = 1 μm, L = 30 m) was maintained at 40°C for 3 min, and was then varied from 40°C to 220°C. It rose from 40°C to 120°C at 5°C·min^{-1}, and then from 120°C to 220°C at 10°C·min^{-1}. Finally, it was maintained at 220°C for 5 min. The total length of the program was 34 min.

Pilot-scale experiments

The systematic experimental studies were performed on experimental pilot devices described in previous articles,[5,21] using commercial hollow fiber membrane contactors (LIQUICEL, Hoechst Celanese, Alting SA, France) made of 10,000 polypropylene fibers. The mean pore diameter of the hollow fiber was 0.03μm. To consider the abnormality of pore shape through the membrane thickness, a tortuosity factor (τ) from 2 to 2.5 is generally considered in the literature for these membranes.[3,25,30] The main characteristics of the two modules are presented in Table 3.

Further details concerning the X-40 module were given by Pierre et al.,[5] while Mahmud et al.[20] gave a detailed description of the X-30 module.

In all experiments, the minimum pressure difference between the two phases was systematically adjusted between 0.5 and 1 bar in order to prevent the dispersion of one phase into the other. It was not accurately monitored since many authors have shown that it has no influence on mass transfer.[3,31]

All the materials used in the test rigs were chosen for their

Table 2. Diffusion Coefficients of the 15 Aroma Compounds of the Model Solution

Molecule	Diffusion Coefficients (m^2 · s^{-1}) at 25°C[a]		
	In Water	In Hexane	In Air
Dimethyldisulfide	$1.1 \cdot 10^{-9}$	$4.4 \cdot 10^{-9}$	$8.7 \cdot 10^{-6}$
Dimethyltrisulfide	$9.7 \cdot 10^{-10}$	$3.9 \cdot 10^{-9}$	$7.7 \cdot 10^{-6}$
Isoamyl alcohol	$9.3 \cdot 10^{-10}$	$3.8 \cdot 10^{-9}$	$8.0 \cdot 10^{-6}$
cis-3-Hexenol	$8.6 \cdot 10^{-10}$	$3.5 \cdot 10^{-9}$	$7.5 \cdot 10^{-6}$
Hexanal	$8.4 \cdot 10^{-10}$	$3.4 \cdot 10^{-9}$	$7.5 \cdot 10^{-6}$
2,5-Dimethylpyrazine	$8.8 \cdot 10^{-10}$	$3.6 \cdot 10^{-9}$	$8.1 \cdot 10^{-6}$
Benzaldehyde	$8.5 \cdot 10^{-10}$	$3.5 \cdot 10^{-9}$	$7.9 \cdot 10^{-6}$
Hexanol	$8.4 \cdot 10^{-10}$	$3.4 \cdot 10^{-9}$	$7.4 \cdot 10^{-6}$
Ethyl butyrate	$8.3 \cdot 10^{-10}$	$3.4 \cdot 10^{-9}$	$7.2 \cdot 10^{-6}$
Isoamyl acetate	$8.3 \cdot 10^{-10}$	$3.4 \cdot 10^{-9}$	$6.7 \cdot 10^{-6}$
2-Heptanone	$7.8 \cdot 10^{-10}$	$3.2 \cdot 10^{-9}$	$7.4 \cdot 10^{-6}$
Ethyl hexanoate	$7.1 \cdot 10^{-10}$	$2.9 \cdot 10^{-9}$	$6.3 \cdot 10^{-6}$
Terpineol	$7.0 \cdot 10^{-10}$	$2.8 \cdot 10^{-9}$	$5.8 \cdot 10^{-6}$
γ-Decalactone	$6.5 \cdot 10^{-10}$	$2.7 \cdot 10^{-9}$	$5.7 \cdot 10^{-6}$
Linalool	$6.4 \cdot 10^{-10}$	$2.6 \cdot 10^{-9}$	$5.8 \cdot 10^{-6}$

[a] Estimated using the Wilke and Chang method.[29]

Table 3. The Main Characteristics of the Liqui-Cel Modules Given by the Manufacturer

Module	MBSE X-40	MAS X-30
Cartridge dimension (cm)	8 × 28	
Effective membrane surface (m^2)	1.4	
Fiber material	Polypropylene	
Housing material	Polyethylene	
Number of fibers	10,000	
Pore diameter (μm)	0.03	
Fiber outer diameter (μm)	300	
Fiber inner diameter (μm)	200	240
Fiber wall thickness (μm)	50	30
Porosity (%)	25	40

inertness toward organic compounds, in order to prevent any mass loss of aroma compounds by sorption (stainless-steel, PTFE, glass). The aqueous feed phase (5L for MBSE experiments or 30L for MAS) and n-hexane (1L) were pumped out of their feed reservoirs, heated to the operating temperature, passed through the module, and circulated back to the same reservoir. Stripping air was distributed in an opened loop. It was first dried and filtered to eliminate water and oils in the distribution system, and then heated to the operating temperature. Temperature (Pt 100, Thermo Est, France) and humidity (Hygroflex, Rotronic, France) sensors at the inlet and at the outlet of the HFC made it possible to control the operating conditions of the air-stripping phase.

According to the results obtained in a previous study,[8] it was decided that the feed phase containing aroma compounds would flow inside the shell compartment, while the stripping phase would flow inside the tube. This configuration has the advantage of offering a larger exchange area for the aroma compounds (1.4 m^2) when compared to the reverse configuration (0.9 m^2).

Samples (1mL) of the aqueous feed phase were taken every 10 min to monitor the extraction kinetics.

Results and Discussion

Experimental results

Partition Coefficients. The determination of theoretical as well as experimental overall mass transfer coefficients assumes that the partition coefficients are known.

The partition coefficient at equilibrium of each solute between water and *n*-hexane was determined at 25°C. Results are presented in Table 4. Pierre et al.[5] showed that partition coefficients of aroma compounds between n-hexane and water were independent of the concentration of the solute in the aqueous feed phase at equilibrium and up to 20 $mg{\cdot}L^{-1}$ (infinite dilution range). Moreover, by determining the partition coefficients of the solutes, either in their pure state or mixed together, they proved that there were no interactive nor competitive effects in the mixture, confirming the infinite dilution range.

For the aroma compounds used in this study, values of the hexane-water partition coefficients range from 1.9 (2,5-dimethylpyrazine) to 1193 (ethyl hexanoate) at 25°C. Partition coefficients are quite well correlated with log P (commonly known as the constant of hydrophobicity, Table 1) since the more hydrophobic the molecule, the more it will have an affinity for n-hexane.

Values of H range from 4.10^{-4} (2,5-dimethylpyrazine) to $6.5.10^{-2}$ (dimethyldisulfide) at 25°C. These values are lower than those for the VOCs usually considered, such as chloroform (H = 0.15 at 23°C) or toluene (H = 0.23 at 23°C), for example, whose extraction was previously studied by Mahmud et al. on a pilot-scale MAS.[32]

Values of H are much smaller than $P_{hexane/water}$ (about 10,000 times), which should make mass transfer less intense in MAS than in MBSE for the same exchange area and the same driving force.

Influence of the Properties of the Molecules on Mass Transfer. Extraction experiments were run on the aroma compounds model solution (aqueous feed) in the two membrane contactor pilot plants. The aqueous feed cross-flowed on the shell side of the membrane (MBSE: $Q_f = 120L{\cdot}h^{-1}$, Re shell = 3.5; MAS: $Q_f = 240L{\cdot}h^{-1}$, Re shell = 7.1), while either air or n-hexane flowed in the lumen of the hollow fibers ($Q_{air} = 600L{\cdot}h^{-1}$, Re fibers = 7.5; $Q_{hexane} = 60L{\cdot}h^{-1}$, Re fibers = 23.3). The overall aqueous feed-based mass-transfer coefficient (K_f, $m{\cdot}s^{-1}$) was determined for each molecule from the extraction kinetics of each aroma compound in the aqueous feed during experiments under fixed hydrodynamic conditions. Experimental values of K_f were plotted against partition coefficients since it was identified as the main physicochemical property responsible for mass transfer[21] (Figure 1).

For the wide range of aroma compounds studied and regardless of the principle chosen to carry out the separation, the higher the partition coefficient, the higher the mass transfer coefficient (K_f, $m{\cdot}s^{-1}$). Mass transfer coefficients varied from 10^{-8} to 7.10^{-6} for MAS under the hydrodynamic conditions of the experiments, while partition coefficients varied from 4.10^{-4} to $6.5.10^{-2}$.

The experimental values of K_f obtained with the MBSE apparatus were generally higher than for MAS, due to higher partition coefficients. K_f ranged from 3.10^{-7} to 2.10^{-4} while partition coefficients ranged from 2 to 1200. For the same range of aroma compounds, it should be observed that the variation in K_f values for MBSE is of the same order of magnitude as for MAS ($K_f^{max}/K_f^{min} \approx 700$), while the variation

Table 4. Experimental Partition Coefficients of the 15 Aroma Compounds of the Model Solution

Molecule	Partition Coefficients (−) at 25°C: Hexane-Water	Air-Water × 10^3
Ethyl hexanoate	1193 ± 102[a]	41 ± 7[d]
Dimethyltrisulfide	560[b]	22 ± 2[d]
Linalool	417 ± 26[a]	2.3 ± 0.3[d]
γ-Decalactone	340 ± 14[a]	0.2 ± 0.1[a]
Isoamyl acetate	304 ± 3[a]	25 ± 3[d]
Terpineol	182 ± 14[a]	0.9 ± 0.2[a]
2-Heptanone	113 ± 2[a]	8.1 ± 0.9[d]
Ethyl butyrate	93.7 ± 0.4[a]	18 ± 2[d]
Dimethyldisulfide	92[b]	65 ± 8[d]
Hexanal	60[c]	22 ± 3[a]
Hexanol	33 ± 8[a]	1.2 ± 0.2[d]
Benzaldehyde	31 ± 8[a]	1.9 ± 0.3[d]
cis-3-Hexenol	10 ± 3[a]	0.4 ± 0.1[a]
Isoamyl alcohol	5.9 ± 0.6[a]	1.0 ± 0.2[d]
2,5-Dimethylpyrazine	1.9 ± 0.5[a]	0.4 ± 0.2[a]

[a] This study.
[b] Pierre et al.[8]
[c] Souchon et al.[6]
[d] Gascons Viladomat et al.[21]

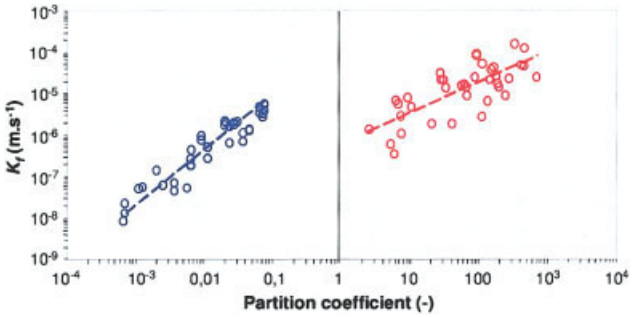

Figure 1. Relation between the overall aqueous-phase-based mass-transfer coefficient (K_f, m·s^{-1}) and the partition coefficient in MAS (left side) and MBSE (right side).

MAS: Re fibers = 7.5, Re shell = 7.1; MBSE: Re fibers = 23.3, Re shell = 3.5. [Color figure can be viewed in the online issue, which is available at www.interscience.wiley.com.]

in partition coefficients is different for each system (($P^{max}/P^{min})_{MBSE} \approx 600$ while $(P^{max}/P^{min})_{MAS} \approx 150$). That means that a variation in partition coefficients will have a stronger impact on mass transfer in MAS than in MBSE. Furthermore, K_f is better correlated to the partition coefficient in MAS than in MBSE (linear relationship with $R^2 = 0.75$ and 0.56, respectively). This could be due to the more rapid extraction rates provided by MBSE, which could lead to more imprecise determinations of the mass transfer coefficients.

Influence of the Hydrodynamic Conditions on Mass Transfer. The influence of the hydrodynamic conditions was studied in order to better compare the mass transfer involved in the two techniques. For this purpose, the concentration of the aroma compounds in the aqueous feed phase was monitored in the two apparatuses under various hydrodynamic conditions of the aqueous feed phase (shell side) and of the stripping phase (fibers), respectively.

Figure 2 shows the evolution of the relative concentration ($C_f(t)/C_f^\circ$) of dimethyldisulfide for two aqueous feed (shell side) flow rates in MBSE. The impact of the hydrodynamic

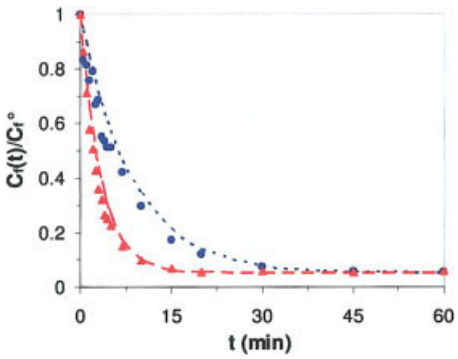

Figure 2. Influence of the aqueous feed phase hydrodynamic conditions on the extraction of dimethyldisulfide in MBSE.

Aqueous feed relative concentration ($C_f(t)/C_f^\circ$) as a function of time (t, min). Re fibers = 25.2, Re shell = 3.8 (▲, – –) Re shell = 1.2 (●, · · · · ·). Curves represent the model prediction. [Color figure can be viewed in the online issue, which is available at www.interscience.wiley.com.]

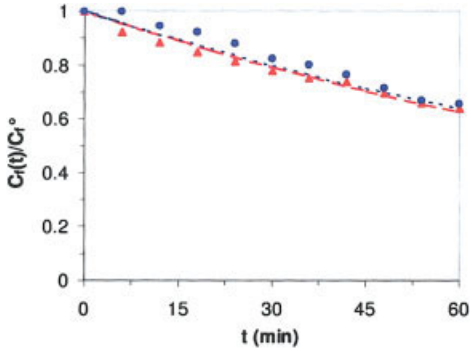

Figure 3. Influence of the aqueous feed phase hydrodynamic conditions on the extraction of dimethyldisulfide in MAS.

Aqueous feed relative concentration ($C_f(t)/C_f^\circ$) as a function of time (t, min). Re fibers = 2.5, Re shell = 14.2 (▲, – –), and Re shell = 1.8 (●, · · · · ·). Curves represent the model prediction. [Color figure can be viewed in the online issue, which is available at www.interscience.wiley.com.]

conditions in the fibers (n-hexane) is not represented since it is not significant.[5] However, this point will be discussed in the model section of this article.

According to Figure 2, the higher the aqueous feed flow rate, the higher the extraction rate, since hydrodynamic conditions are more favorable.

Figure 3 represents the evolution of the relative concentration in the aqueous feed of dimethyldisulfide for two aqueous feed flow rates in MAS. In this case, the aqueous feed flow rate has a negligible impact on mass transfer. Figure 4 shows the impact of the air-stripping flow rate on mass transfer. As shown by Souchon et al.,[26] an increase in the air-stripping flow rate leads to higher extraction rates. This enhancement of extraction kinetics results from two distinct phenomena. The increase of the air flow-rate leads to: (1) more favorable hydrodynamic conditions (lower boundary layer thickness), and (2) a higher extraction capacity due to a greater amount of air flowing in the module for a given time, since air flows in an open loop. But the stripping phase is more diluted in aroma compounds, making the recovery more difficult.

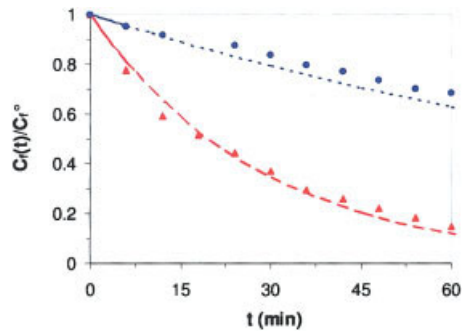

Figure 4. Influence of the air-stripping phase hydrodynamic conditions on the extraction of dimethyldisulfide in MAS.

Aqueous feed relative concentration ($C_f(t)/C_f^\circ$) as a function of time (t, min). Re shell = 7.1, Re fibers = 12.5 (▲, – –), and Re fibers = 2.5 (●, · · · · ·). Curves represent the model prediction. [Color figure can be viewed in the online issue, which is available at www.interscience.wiley.com.]

Figures 2, 3, and 4 show that mass transfer can be enhanced by increasing the aqueous feed flow rate in MBSE or by increasing the stripping phase flow rate in MAS. This difference in the behavior of the two processes should be explained by the position of the limiting step for mass transfer (in the aqueous feed boundary layer, in the membrane, or in the stripping phase film). The resistance-in-series model will allow the identification of this limiting step by the estimation of each local resistance to mass transfer.

Modeling of mass transfer

The resistance-in-series model was used for the prediction of the relative aqueous feed concentrations of dimethyldisulfide as a function of time in MBSE and MAS extraction experiments.

Figures 2, 3, and 4 show that the results given by the model are close to experimental values regardless of the hydrodynamic conditions for the two technologies.

Since the model well described the behavior of a single molecule for various hydrodynamic conditions, it was then used to predict mass transfer of molecules with various physicochemical properties.

Figures 5 and 6 show both experimental results and the results given by the model for isoamyl acetate, 2-heptanone, and benzaldehyde. These molecules were chosen for these representations because of the considerable differences in their physicochemical properties. Isoamyl acetate is highly hydrophobic ($P_{hexane/water}$=304) and relatively highly volatile ($H = 2.5.10^{-2}$), benzaldehyde is weakly hydrophobic ($P_{hexane/water} = 31$) and has a low volatility ($H = 1.9.10^{-3}$), whereas 2-heptanone is somewhere in between ($P_{hexane/water} = 113$ and $H = 8.1.10^{-3}$).

Under given hydrodynamic conditions, global mass transfer coefficients provided by the model are close to experimental ones for the whole range of physicochemical properties ($P_{hexane/water}$ and H). It should be noticed that partition coefficients have a much stronger impact on mass transfer for MAS than for MBSE. Under given hydrodynamic conditions, increasing $P_{hexane/water}$ from 31 to 304 (10 times) leads to an increase in K_f from $2.0.10^{-5}$ m·s^{-1} to $2.3.10^{-5}$ m·s^{-1} (1.15 times). However, increasing H from $1.9.10^{-3}$ to $2.5.10^{-2}$ (13 times) leads to an increase in K_f from $3.3.10^{-7}$ m·s^{-1} to $3.9.10^{-6}$ m·s^{-1} (12 times). This makes MAS much more selective than MBSE.

The model effectively takes both hydrodynamic conditions and physicochemical properties of the molecules into account. As a result, it was interesting to study this phenomenon more extensively by predicting the evolution of the global mass transfer coefficient on the basis of hydrodynamic conditions for the three molecules.

Figure 5 shows the evolution of K_f on the basis of the hydrodynamic conditions on the shell side for isoamyl acetate, 2-heptanone, and benzaldehyde.

For MBSE, the higher the Reynolds number on the shell side, the higher the overall mass transfer coefficient, regardless of the molecule. However, as was previously seen, mass transfer coefficients are very similar from one molecule to the next.

Concerning MAS, the global mass transfer coefficient increases with the Reynolds number for only very small Re (Re < 2), in the case of isoamyl acetate. For benzaldehyde, no evolution can be observed.

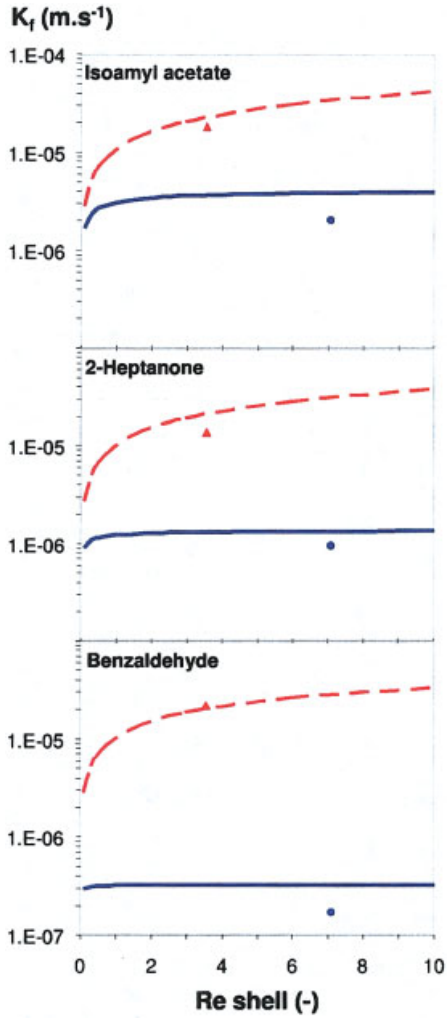

Figure 5. Influence of the hydrodynamic conditions of the shell side (Re shell, -) on the overall aqueous-feed-based mass-transfer coefficient (K_f, m·s^{-1}).

MBSE (▲experimental, – – model prediction) and MAS (●experimental, ▬ model prediction). Re fibers = 23.3 and 7.5 for MBSE and MAS, respectively. [Color figure can be viewed in the online issue, which is available at www.interscience.wiley.com.]

When changing the Reynolds number in the fibers (Figure 6), mass transfer does not change for MBSE, while K_f increases when increasing the Reynolds number for MAS.

Table 5 shows the contribution of each local resistance ($R_i = 1/k_i$, s·m^{-1}) to the global resistance ($R = 1/K_f$) for the three characteristic compounds. For the most hydrophobic molecule (isoamyl acetate), more than 98% of the resistance is located in the aqueous feed boundary layer in MBSE. For the least hydrophobic molecule, this contribution drops to 86%. It should be noticed that the contribution of the membrane in this case is more than 11%, which is not negligible.

In MAS, more than 98% of the resistance is located in the gas film for benzaldehyde (the least volatile), while it is 88% for isoamyl acetate (the most volatile). In the case of MAS, the membrane never contributes to more than 0.5% of the global resistance.

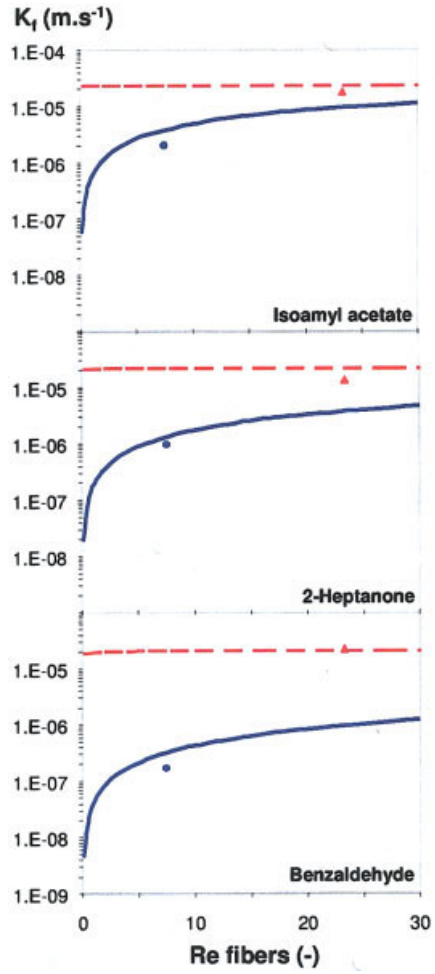

Figure 6. Influence of the hydrodynamic conditions in the fibers (Re fibers, -) on the overall aqueous-feed-based mass-transfer coefficient (K_f, m·s^{-1}).

MBSE (▲experimental, – – model prediction) and MAS (●experimental, ▬ model prediction). Re shell = 3.5 and 7.1 for MBSE and MAS, respectively. [Color figure can be viewed in the online issue, which is available at www.interscience.wiley.com.]

Figure 7 shows the distribution of local resistances to mass transfer for the 15 molecules studied in the model solution in MAS. For the least volatile molecules, the resistance in the aqueous boundary layer is negligible because of the high value of the resistance in the gas boundary layer. However, for $H > 1.10^{-2}$, the resistance in the gas boundary layer starts to decrease, leading to an increase in the contribution of the aqueous feed boundary layer, but a global decrease of K_f.

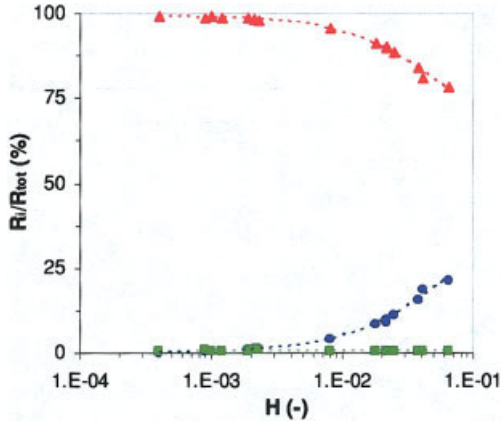

Figure 7. Influence of aroma compound volatility (H, -) on the contribution of local resistances to mass transfer (R_i/R_{tot}, -) in MAS.

●: Aqueous feed boundary layer, ■: membrane, ▲: gas boundary layer. Re fibers = 7.5, Re shell = 7.1. [Color figure can be viewed in the online issue, which is available at www.interscience.wiley.com.]

A similar figure is shown for MBSE (Figure 8). In this case, the main resistance to mass transfer is located in the aqueous boundary layer for the most hydrophobic molecules. However, for the less hydrophobic molecules, the membrane becomes the preponderant resistance to mass transfer.

As a conclusion, the contribution of each area of the membrane contactor to resistance to mass transfer was identified. It is dependent on the hydrodynamic conditions and the physicochemical properties of the molecules, regardless of the extraction principle (MBSE or MAS).

Physicochemical diagnosis

It was shown in this article that the physicochemical properties of the molecules had a strong impact on mass transfer. By determining the ratio (K_f^{MBSE}/K_f^{MAS}), we can determine the relative benefits of using a technology for a given molecule.

Table 6 confirms that mass transfer is higher in MBSE than in MAS. For molecules that are hydrophobic but not volatile (such as terpene alcohols), K_f^{MBSE} can be more than 1000 times higher than K_f^{MAS}. Consequently, extracting such molecules is much more favorable with MBSE than with MAS.

However, in addition to the mass transfer performances of a technology, other parameters need to be taken into account when choosing a separation process. It would, therefore, be

Table 5. Contribution of the Local Resistances to the Global Resistance (R_i/R_{tot})

Molecule			Overall Resistance Contribution (%)		
			Aqueous	Membrane	Solvent/Gas
Isoamyl acetate	$P_{hexane/water}$ (−)	304	98.4	1.3	0.3
	$H \times 10^3$ (−)	25.0	11.2	0.5	88.3
2-Heptanone	$P_{hexane/water}$ (−)	113	95.7	3.6	0.7
	$H \times 10^3$ (−)	8.1	4.1	0.5	95.4
Benzaldehyde	$P_{hexane/water}$ (−)	31	86.3	11.4	2.4
	$H \times 10^3$ (−)	1.9	0.9	0.5	98.6

MBSE: Re shell = 3.5, Re fibers = 23.3 − MAS: Re shell = 7.1, Re fibers = 7.5.

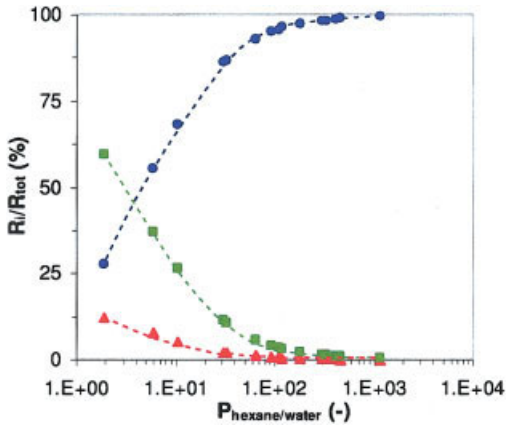

Figure 8. Influence of aroma compound affinity for the organic solvent ($P_{hexane/water}$, -) on the contribution of local resistances to mass transfer (R_i/R_{tot}, -) in MBSE.

●: Aqueous feed boundary layer, ■: membrane, ▲: solvent boundary layer. Re fibers = 23.3, Re shell = 3.5. [Color figure can be viewed in the online issue, which is available at www.interscience.wiley.com.]

interesting to implement a method allowing the determination of a threshold value for (K_f^{MBSE}/K_f^{MAS}), that would take the constraints of the application (required efficiency and/or selectivity), environmental considerations, and, last but not least, economics, into account. For example, in the food industry, the use of a potentially harmful organic solvent would be avoided as much as possible. In this case, (K_f^{MBSE}/K_f^{MAS}) would be relatively high. On the contrary, if maximum efficiency were required, it would be low, regardless of the selectivity of the operation.

For the application studied in this work, (K_f^{MBSE}/K_f^{MAS}) could be attributed the value of 20, considering that the aroma compounds need a further separation from the solvent in MBSE, whereas in MAS, they can be recovered by condensation.[21] Table 6 shows values of (K_f^{MBSE}/K_f^{MAS}) for representative molecules of the model solution. It appears that the discriminating factor is in this case the air-liquid partition coefficient H. If H is low ($H < 3.10^{-3}$, such as terpene alcohols, alcohols), it would, therefore, be better to use MBSE; whereas if H is intermediate to relatively high ($H > 15.10^{-3}$, such as esters, sulfur compounds), MAS would be the better-adapted technology.

Conclusions

The extraction of aroma compounds with hollow fiber contactors from a highly diluted aqueous stream was studied. Two separation principles were compared: Membrane-Based Solvent Extraction (MBSE) and Membrane Air-Stripping (MAS). It appeared that MBSE generally resulted in higher extraction rates than MAS for the aroma compounds in this study. However, MAS does not require the use of an organic solvent and can thus be considered as a clean technology. Mass transfer that takes place in the two systems was modeled using a resistance-in-series approach. The model made it possible to identify the limiting steps for mass transfer: the aqueous boundary layer is the limiting step in MBSE, while the gas boundary layer is the limiting step in MAS. This difference arises from the partition coefficients of the aroma compounds, which have been identified as the main physicochemical property with an impact on mass transfer. Partition coefficients have consequently been used as a key parameter in the establishment of a diagnosis, which could help in choosing the adequate technology for a given separation.

Acknowledgments

The authors express their sincere thanks to Dr. C. Dean, U. Jenelten, and B. Müller (Firmenich S.A., 1 route des Jeunes, CH1211 Geneva 8, Switzerland) for their scientific collaboration and fruitful comments. The authors would also like to thank Firmenich S.A. for financial support. The authors are also indebted to G. Wagman for revising the English version of the manuscript.

Notation

a = surface to volume ratio, $m^2 \cdot m^{-3}$
A = surface area, m^2
BP = boiling point at normal pressure, °C
C = concentration, $kg \cdot m^{-3}$
d = diameter, m
d_h = hydraulic diameter of the hollow fiber, m
D = diffusion coefficient, $m^2 \cdot s^{-1}$
e = membrane thickness, m
Gz = Graetz number
H = Henry's law constant, $kg \cdot m^{-3}/kg \cdot m^{-3}$
k = local mass transfer, $m \cdot s^{-1}$
K_f = overall liquid-based mass transfer coefficient, $m \cdot s^{-1}$
$\dot{m}$ = mass transfer flux, $kg \cdot s^{-1}$
MW = molecular weight, $g \cdot mol^{-1}$
P = partition coefficient
Q = flow rate, $m^3 \cdot s^{-1}$
R = resistance to mass transfer, $s \cdot m^{-1}$
Re = Reynolds number
Sc = Schmidt number

Table 6. Diagnosis Based on the Physicochemical Properties of the Molecules

Chemical Class	Molecule	$P_{hexane/water}$ (−)	$H \times 10^3$ (−)	K_f^{MBSE}/K_f^{MAS} (−)	Diagnosis
Esters	Ethyl hexanoate	1193	41	19	MAS (+)
	Ethyl butyrate	93.7	18	12	
Sulfur compounds	Dimethyltrisulfide	560	22	15	MAS (+)
	Dimethyldisulfide	92	65	13	
Terpene alcohols	Linalool	417	2.3	252	MBSE (++ to +++)
	Terpineol	182	0.9	1429	
Alcohols	Hexanol	33.2	1.2	76	MBSE (+)
	Isoamyl alcohol	5.93	1.0	34	

MBSE: Re shell = 3.5, Re fibers = 23.3 − MAS: Re shell = 7.1, Re fibers = 7.5.
(+): favorable; (++): very favorable; (+++), extremely favorable.

T = temperature, °C
t = time, min
u = velocity, $m \cdot s^{-1}$

Greek letters

ε = membrane porosity
μ = dynamic viscosity, $kg \cdot m^{-1} \cdot s^{-1}$
τ = membrane tortuosity
ν = kinematic viscosity, $m^2 \cdot s^{-1}$

Subscripts

f = aqueous feed phase
m = membrane
s = stripping phase

Superscripts

° = initial value
- = mean value

Literature Cited

1. Gascons Viladomat F, Souchon I, Marin M. Les techniques de séparation pour l'extraction/concentration de molécules odorantes en solution. *Ind Alim Agric*. 2005; 122(9):8–15.
2. Gabelman A, Hwang S-T. Hollow fiber membrane contactors. *J Membrane Sci.* 1999;159:61-106.
3. Kiani A, Bhave RR, Sirkar KK. Solvent extraction with immobilized interfaces in a microporous hydrophobic membrane. *J Membrane Sci.* 1984;20:125-145.
4. Cooney DO, Jin C-L. Solvent extraction of phenol from aqueous solution in a hollow-fiber device. *Chem Eng Commun*. 1985;37:173.
5. Pierre F-X, Souchon I, Marin M. Recovery of sulfur aroma compounds using membrane-based solvent extraction. *J Membrane Sci.* 2001;187: 239-253.
6. Souchon I, Pierre F-X, Samblat S, Bes M, Marin M. Recovery of aroma compounds from tomato industry effluent using membrane-based solvent extraction. *Desalination*. 2002;148:87-92.
7. Baudot A, Floury J, Smorenburg HE. Liquid-liquid extraction of aroma compounds with hollow fiber contactor. *AIChE J.* 2001;47(8): 1780-1793.
8. Pierre F-X, Souchon I, Athès-Dutour V, Marin M. Membrane-based extraction of sulfur aroma compounds: influence of operating conditions on mass transfer coefficients in a hollow fiber contactor. *Desalination.* 2002;148:199-204.
9. Zander AK, Semmens MJ, Narbaitz RM. Removing VOCs by membrane stripping. *J Am Water Works Assoc.* 1989;November:76-81.
10. Semmens MJ, Qin R, Zander AK. Using a microporous hollow-fiber membrane to separate VOCs from Water. *J Am Water Works Assoc.* 1989;April:162-167.
11. Mahmud H, Kumar A, Narbaitz RM, Matsuura T. The air-phase mass transfer resistance in the lumen of a hollow fiber at low air flow. *Chem Eng J.* 2004;97:69-75.
12. Juang R-S, Lin S-H, Yang M-C. Mass transfer analysis on air stripping of VOCs from water in microporous hollow fibers. *J Membrane Sci.* 2005;255:79-87.
13. Robinson JR, Sims MJ. U.S. Patent No. 5 490 884; 1996.
14. Bothun GD, Knutson BL, Strobel HJ, Nokes SE. Mass transfer in hollow fiber contactor extraction using compressed solvents. *J Membrane Sci.* 2003;227:183-196.
15. Gabelman A, Hwang S-T, Krantz WB. Dense gas extraction using a hollow fiber membrane contactor: experimental results versus model predictions. *J Membrane Sci.* 2005;257:11-36.
16. D'Elia NA, Dahuron L, Cussler EL. Liquid-liquid extractions with microporous hollow fibers. *J Membrane Sci.* 1986;29:309-319.
17. Mahmud H, Kumar A, Narbaitz RM, Matsuura T. Membrane air stripping: a process for removal of organics from aqueous solutions. *Sep Sci & Technol.* 1998;33(14):2241-2255.
18. Kreith F, Black WZ. *Basic Heat Transfer.* New York: Harper & Row; 1980.
19. Bocquet S, Gascons Viladomat F, Muvdi Nova C, Sanchez J, Athès V, Souchon I. Membrane-based solvent extraction of aroma compounds: choice of configurations of hollow fiber modules based on experiments and simulation. *J Membrane Sci.* Submitted.
20. Mahmud H, Kumar A, Narbaitz RM, Matsuura T. A study of mass transfer in the membrane air-stripping process using microporous polypropylene hollow fibers. *J Membrane Sci.* 2000;179:29-41.
21. Gascons Viladomat F, Souchon I, Athès V, Marin M. Membrane air-stripping of aroma compounds. *J Membrane Sci.* in press (available online, as corrected proof).
22. Graetz L. Über die wärmeleitungsfähigkeit von flüssigkeiten. *Ann Phys Chem.* 1885;25: 337-357.
23. Lévêque MA. Les lois de la transmission de chaleur par convection. *Ann Mines.* 1928;13:201-299.
24. Viegas RMC, Rodriguez M, Luque S, Alvarez JR, Coelhoso IM, Crespo JPSG. Mass transfer correlations in membrane extraction: analysis of Wilson-plot methodology. *J Membrane Sci.* 1998;145:129-142.
25. Prasad R, Sirkar KK. Dispersion-free solvent extraction with microporous hollow-fiber modules. *AIChE J.* 1988;34(2):177-187.
26. Souchon I, Athès V, Pierre F-X, Marin M. Liquid-liquid extraction and air stripping in membrane contactor: application to aroma compounds recovery. *Desalination.* 2004;63:39-46.
27. EPI suite V3.10 (US Environmental Protection Agency). Estimation Programs Interface (EPI) Suite™ V.3.10. (2000): Environmental Protection Agency, EPA's Office of Pollution Prevention Toxics and Syracuse Research Corporation (SRC).
28. Ettre LS, Welter C, Kolb B. Determination of gas-liquid partition coefficients by automatic equilibrium head-space gas chromatography utilizing phase ratio variation method. *Chromatographia.* 1993;35:73-84.
29. Reid RC, Prausnitz JM, Poling BE. *The Properties of Gases and Liquids.* New York: McGraw-Hill, Inc.; 1987.
30. Schöner P, Plucinski P, Nitsch W, Daiminger U. Mass transfer in the shell side of cross flow hollow fiber modules. *Chem Eng Sci.* 1998; 53:2319-2326.
31. Prasad R, Bhave RR, Kiani AK, Sirkar KK. Further studies on solvent extraction with immobilized interfaces in a microporous hydrophobic membrane. *J Membrane Sci.* 1986;26:79-97.
32. Mahmud H, Kumar A., Narbaitz RM, Matsuura T. Mass transport in the membrane air-stripping process using microporous polypropylene hollow fibers: effect of toluene in aqueous feed. *J Membrane Sci.* 2002;209:207-219.

Manuscript received Nov. 14, 2005, and revision received Feb. 15, 2006.